

NMR SPECTROSCOPY EXPLAINED

Simplified Theory, Applications and Examples for Organic Chemistry and Structural Biology

Neil E. Jacobsen, Ph.D.
University of Arizona



**WILEY-
INTERSCIENCE**

A JOHN WILEY & SONS, INC., PUBLICATION

NMR SPECTROSCOPY EXPLAINED



THE WILEY BICENTENNIAL—KNOWLEDGE FOR GENERATIONS

Each generation has its unique needs and aspirations. When Charles Wiley first opened his small printing shop in lower Manhattan in 1807, it was a generation of boundless potential searching for an identity. And we were there, helping to define a new American literary tradition. Over half a century later, in the midst of the Second Industrial Revolution, it was a generation focused on building the future. Once again, we were there, supplying the critical scientific, technical, and engineering knowledge that helped frame the world. Throughout the 20th Century, and into the new millennium, nations began to reach out beyond their own borders and a new international community was born. Wiley was there, expanding its operations around the world to enable a global exchange of ideas, opinions, and know-how.

For 200 years, Wiley has been an integral part of each generation's journey, enabling the flow of information and understanding necessary to meet their needs and fulfill their aspirations. Today, bold new technologies are changing the way we live and learn. Wiley will be there, providing you the must-have knowledge you need to imagine new worlds, new possibilities, and new opportunities.

Generations come and go, but you can always count on Wiley to provide you the knowledge you need, when and where you need it!

WILLIAM J. PESCE
PRESIDENT AND CHIEF EXECUTIVE OFFICER

PETER BOOTH WILEY
CHAIRMAN OF THE BOARD

NMR SPECTROSCOPY EXPLAINED

Simplified Theory, Applications and Examples for Organic Chemistry and Structural Biology

Neil E. Jacobsen, Ph.D.
University of Arizona



**WILEY-
INTERSCIENCE**

A JOHN WILEY & SONS, INC., PUBLICATION

Copyright © 2007 by John Wiley & Sons, Inc. All rights reserved

Published by John Wiley & Sons, Inc., Hoboken, New Jersey
Published simultaneously in Canada

No part of this publication may be reproduced, stored in a retrieval system, or transmitted in any form or by any means, electronic, mechanical, photocopying, recording, scanning, or otherwise, except as permitted under Section 107 or 108 of the 1976 United States Copyright Act, without either the prior written permission of the Publisher, or authorization through payment of the appropriate per-copy fee to the Copyright Clearance Center, Inc., 222 Rosewood Drive, Danvers, MA 01923, (978) 750-8400, fax (978) 750-4470, or on the web at www.copyright.com. Requests to the Publisher for permission should be addressed to the Permissions Department, John Wiley & Sons, Inc., 111 River Street, Hoboken, NJ 07030, (201) 748-6011, fax (201) 748-6008, or online at <http://www.wiley.com/go/permission>.

Limit of Liability/Disclaimer of Warranty: While the publisher and author have used their best efforts in preparing this book, they make no representations or warranties with respect to the accuracy or completeness of the contents of this book and specifically disclaim any implied warranties of merchantability or fitness for a particular purpose. No warranty may be created or extended by sales representatives or written sales materials. The advice and strategies contained herein may not be suitable for your situation. You should consult with a professional where appropriate. Neither the publisher nor author shall be liable for any loss of profit or any other commercial damages, including but not limited to special, incidental, consequential, or other damages.

For general information on our other products and services or for technical support, please contact our Customer Care Department within the United States at (800) 762-2974, outside the United States at (317) 572-3993 or fax (317) 572-4002.

Wiley also publishes its books in a variety of electronic formats. Some content that appears in print may not be available in electronic formats. For more information about Wiley products, visit our web site at <http://www.wiley.com>.

Wiley Bicentennial Logo: Richard J. Pacifico

Library of Congress Cataloging-in-Publication Data:

Jacobsen, Neil E.

NMR Spectroscopy Explained : Simplified Theory, Applications and Examples for Organic Chemistry and Structural Biology / Neil E Jacobsen, Ph.D.

p. cm.

ISBN 978-0-471-73096-5 (cloth)

1. Nuclear magnetic resonance spectroscopy. 2. Chemistry, Organic. 3. Molecular biology. I. Title.

QD96.N8J33 2007

543'.66- -dc22

2007006911

Printed in the United States of America

10 9 8 7 6 5 4 3 2 1

CONTENTS

Preface	xi
Acknowledgments	xv
1 Fundamentals of NMR Spectroscopy in Liquids	1
1.1 Introduction to NMR Spectroscopy, 1	
1.2 Examples: NMR Spectroscopy of Oligosaccharides and Terpenoids, 12	
1.3 Typical Values of Chemical Shifts and Coupling Constants, 27	
1.4 Fundamental Concepts of NMR Spectroscopy, 30	
2 Interpretation of Proton (¹H) NMR Spectra	39
2.1 Assignment, 39	
2.2 Effect of B_0 Field Strength on the Spectrum, 40	
2.3 First-Order Splitting Patterns, 45	
2.4 The Use of ¹ H- ¹ H Coupling Constants to Determine Stereochemistry and Conformation, 52	
2.5 Symmetry and Chirality in NMR, 54	
2.6 The Origin of the Chemical Shift, 56	
2.7 <i>J</i> Coupling to Other NMR-Active Nuclei, 61	
2.8 Non-First-Order Splitting Patterns: Strong Coupling, 63	
2.9 Magnetic Equivalence, 71	
3 NMR Hardware and Software	74
3.1 Sample Preparation, 75	
3.2 Sample Insertion, 77	
3.3 The Deuterium Lock Feedback Loop, 78	

3.4	The Shim System, 81	
3.5	Tuning and Matching the Probe, 88	
3.6	NMR Data Acquisition and Acquisition Parameters, 90	
3.7	Noise and Dynamic Range, 108	
3.8	Special Topic: Oversampling and Digital Filtering, 110	
3.9	NMR Data Processing—Overview, 118	
3.10	The Fourier Transform, 119	
3.11	Data Manipulation Before the Fourier Transform, 122	
3.12	Data Manipulation After the Fourier Transform, 126	
4	Carbon-13 (¹³C) NMR Spectroscopy	135
4.1	Sensitivity of ¹³ C, 135	
4.2	Splitting of ¹³ C Signals, 135	
4.3	Decoupling, 138	
4.4	Heteronuclear Decoupling: ¹ H Decoupled ¹³ C Spectra, 139	
4.5	Decoupling Hardware, 145	
4.6	Decoupling Software: Parameters, 149	
4.7	The Nuclear Overhauser Effect (NOE), 150	
4.8	Heteronuclear Decoupler Modes, 152	
5	NMR Relaxation—Inversion-Recovery and the Nuclear Overhauser Effect (NOE)	155
5.1	The Vector Model, 155	
5.2	One Spin in a Magnetic Field, 155	
5.3	A Large Population of Identical Spins: Net Magnetization, 157	
5.4	Coherence: Net Magnetization in the <i>x</i> - <i>y</i> Plane, 161	
5.5	Relaxation, 162	
5.6	Summary of the Vector Model, 168	
5.7	Molecular Tumbling and NMR Relaxation, 170	
5.8	Inversion-Recovery: Measurement of <i>T</i> ₁ Values, 176	
5.9	Continuous-Wave Low-Power Irradiation of One Resonance, 181	
5.10	Homonuclear Decoupling, 182	
5.11	Presaturation of Solvent Resonance, 185	
5.12	The Homonuclear Nuclear Overhauser Effect (NOE), 187	
5.13	Summary of the Nuclear Overhauser Effect, 198	
6	The Spin Echo and the Attached Proton Test (APT)	200
6.1	The Rotating Frame of Reference, 201	
6.2	The Radio Frequency (RF) Pulse, 203	
6.3	The Effect of RF Pulses, 206	
6.4	Quadrature Detection, Phase Cycling, and the Receiver Phase, 209	

6.5	Chemical Shift Evolution, 212	
6.6	Scalar (J) Coupling Evolution, 213	
6.7	Examples of J -coupling and Chemical Shift Evolution, 216	
6.8	The Attached Proton Test (APT), 220	
6.9	The Spin Echo, 226	
6.10	The Heteronuclear Spin Echo: Controlling J -Coupling Evolution and Chemical Shift Evolution, 232	
7	Coherence Transfer: INEPT and DEPT	238
7.1	Net Magnetization, 238	
7.2	Magnetization Transfer, 241	
7.3	The Product Operator Formalism: Introduction, 242	
7.4	Single Spin Product Operators: Chemical Shift Evolution, 244	
7.5	Two-Spin Operators: J -coupling Evolution and Antiphase Coherence, 247	
7.6	The Effect of RF Pulses on Product Operators, 251	
7.7	INEPT and the Transfer of Magnetization from ^1H to ^{13}C , 253	
7.8	Selective Population Transfer (SPT) as a Way of Understanding INEPT Coherence Transfer, 257	
7.9	Phase Cycling in INEPT, 263	
7.10	Intermediate States in Coherence Transfer, 265	
7.11	Zero- and Double-Quantum Operators, 267	
7.12	Summary of Two-Spin Operators, 269	
7.13	Refocused INEPT: Adding Spectral Editing, 270	
7.14	DEPT: Distortionless Enhancement by Polarization Transfer, 276	
7.15	Product Operator Analysis of the DEPT Experiment, 283	
8	Shaped Pulses, Pulsed Field Gradients, and Spin Locks: Selective 1D NOE and 1D TOCSY	289
8.1	Introducing Three New Pulse Sequence Tools, 289	
8.2	The Effect of Off-Resonance Pulses on Net Magnetization, 291	
8.3	The Excitation Profile for Rectangular Pulses, 297	
8.4	Selective Pulses and Shaped Pulses, 299	
8.5	Pulsed Field Gradients, 301	
8.6	Combining Shaped Pulses and Pulsed Field Gradients: “Excitation Sculpting”, 308	
8.7	Coherence Order: Using Gradients to Select a Coherence Pathway, 316	
8.8	Practical Aspects of Pulsed Field Gradients and Shaped Pulses, 319	
8.9	1D Transient NOE using DPFGE, 321	
8.10	The Spin Lock, 333	
8.11	Selective 1D ROESY and 1D TOCSY, 338	
8.12	Selective 1D TOCSY using DPFGE, 343	
8.13	RF Power Levels for Shaped Pulses and Spin Locks, 348	

9	Two-Dimensional NMR Spectroscopy: HETCOR, COSY, and TOCSY	353
9.1	Introduction to Two-Dimensional NMR,	353
9.2	HETCOR: A 2D Experiment Created from the 1D INEPT Experiment,	354
9.3	A General Overview of 2D NMR Experiments,	364
9.4	2D Correlation Spectroscopy (COSY),	370
9.5	Understanding COSY with Product Operators,	386
9.6	2D TOCSY (Total Correlation Spectroscopy),	393
9.7	Data Sampling in t_1 and the 2D Spectral Window,	398
10	Advanced NMR Theory: NOESY and DQF-COSY	408
10.1	Spin Kinetics: Derivation of the Rate Equation for Cross-Relaxation,	409
10.2	Dynamic Processes and Chemical Exchange in NMR,	414
10.3	2D NOESY and 2D ROESY,	425
10.4	Expanding Our View of Coherence: Quantum Mechanics and Spherical Operators,	439
10.5	Double-Quantum Filtered COSY (DQF-COSY),	447
10.6	Coherence Pathway Selection in NMR Experiments,	450
10.7	The Density Matrix Representation of Spin States,	469
10.8	The Hamiltonian Matrix: Strong Coupling and Ideal Isotropic (TOCSY) Mixing,	478
11	Inverse Heteronuclear 2D Experiments: HSQC, HMQC, and HMBC	489
11.1	Inverse Experiments: ^1H Observe with ^{13}C Decoupling,	490
11.2	General Appearance of Inverse 2D Spectra,	498
11.3	Examples of One-Bond Inverse Correlation (HMQC and HSQC) Without ^{13}C Decoupling,	501
11.4	Examples of Edited, ^{13}C -Decoupled HSQC Spectra,	504
11.5	Examples of HMBC Spectra,	509
11.6	Structure Determination Using HSQC and HMBC,	517
11.7	Understanding the HSQC Pulse Sequence,	522
11.8	Understanding the HMQC Pulse Sequence,	533
11.9	Understanding the Heteronuclear Multiple-Bond Correlation (HMBC) Pulse Sequence,	535
11.10	Structure Determination by NMR—An Example,	538
12	Biological NMR Spectroscopy	551
12.1	Applications of NMR in Biology,	551
12.2	Size Limitations in Solution-State NMR,	553
12.3	Hardware Requirements for Biological NMR,	558
12.4	Sample Preparation and Water Suppression,	564
12.5	^1H Chemical Shifts of Peptides and Proteins,	570

12.6	NOE Interactions Between One Residue and the Next Residue in the Sequence, 577	
12.7	Sequence-Specific Assignment Using Homonuclear 2D Spectra, 580	
12.8	Medium and Long-Range NOE Correlations, 586	
12.9	Calculation of 3D Structure Using NMR Restraints, 590	
12.10	¹⁵ N-Labeling and 3D NMR, 596	
12.11	Three-Dimensional NMR Pulse Sequences: 3D HSQC–TOCSY and 3D TOCSY–HSQC, 601	
12.12	Triple-Resonance NMR on Doubly-Labeled (¹⁵ N, ¹³ C) Proteins, 610	
12.13	New Techniques for Protein NMR: Residual Dipolar Couplings and Transverse Relaxation Optimized Spectroscopy (TROSY), 621	
	Appendix A: A Pictorial Key to NMR Spin States	627
	Appendix B: A Survey of Two-Dimensional NMR Experiments	634
	Index	643

PREFACE

Nuclear magnetic resonance (NMR) is a technique for determining the structure of organic molecules and biomolecules in solution. The covalent structure (what atoms are bonded to what), the stereochemistry (relative orientation of groups in space), and the conformation (preferred bond rotations or folding in three dimensions) are available by techniques that measure direct distances (between hydrogens) and bond dihedral angles. Specific NMR signals can be identified and assigned to each hydrogen (and/or carbon, nitrogen) in the molecule.

You may have seen or been inside an MRI (magnetic resonance imaging) instrument, a medical tool that creates detailed images (or “slices”) of the patient without ionizing radiation. The NMR spectroscopy magnet is just a scaled-down version of this huge clinical magnet, rotated by 90° so that the “bore” (the hole that the patient gets into) is vertical and typically only 5 cm (2 in.) in diameter. Another technique, solid-state NMR, deals with solid (powdered) samples and gives information similar to solution NMR. This book is limited to solution-state NMR and will not cover the fields of NMR imaging and solid-state NMR, even though the theoretical tools developed here can be applied to these fields.

NMR takes advantage of the magnetic properties of the nucleus to sense the proximity of electronegative atoms, double bonds, and other magnetic nuclei nearby in the molecular structure. About one half of a micromole of a pure molecule in 0.5 mL of solvent is required for this nondestructive test. Precise structural information down to each atom and bond in the molecule can be obtained, information rivaled only by X-ray crystallography. Because the measurement can be made in aqueous solution, we can also study the effects of temperature, pH, and interactions with ligands and other biomolecules. Uniform labeling (^{13}C , ^{15}N) permits the study of large biomolecules, such as proteins and nucleic acids, up to 30 kD and beyond.

Compared to other analytical techniques, NMR is quite insensitive. For molecules of the size of most drugs and natural products (100–600 Da), about a milligram of pure material is required, compared to less than 1 μg for mass spectrometry. The intensity of NMR signals is directly proportional to concentration, so NMR “sees all” and “tells all,” even

giving multiple signals for stereoisomers or slowly interconverting conformations. This complexity is very rich in information, but it makes mixtures very difficult to analyze. Finally, the NMR instrument is quite expensive (from US \$200,000 to more than \$5 million depending on the magnet strength) and can only analyze one sample at a time, with some experiments requiring a few minutes and the most complex ones requiring up to 4 days to acquire the data. But used in concert with complementary analytical techniques, such as light spectroscopy and mass spectrometry, NMR is the most powerful tool by far for the determination of organic structure. Only X-ray crystallography can give a comparable kind of detailed information on the precise location of atoms and bonds within a molecule.

The kind of information NMR gives is always “local”: The world is viewed from the point of view of one atom in a molecule, and it is a very myopic view indeed: This atom can “see” only about 5 Å or three bonds away (a typical C–H bond is about 1 Å or 0.1 nm long). But the point of view can be moved around so that we “see” the world from each atom in the molecule in turn, as if we could carry a weak flashlight around in a dark room and try to put together a picture of the whole room. The information obtained is always coded and requires a complex (but very satisfying) puzzle-solving exercise to decode it and produce a three-dimensional model of a molecule. In this sense, NMR does not produce a direct “picture” of the molecule like an electron microscope or an electron density map obtained from X-ray crystallography. The NMR data are a set of relationships among the atoms of the molecule, relationships of proximity either directly through space or along the bonding network of the molecule. With a knowledge of these relationships, we can construct an unambiguous model of the molecular structure. To an organic chemist trained in the interpretation of NMR data, this process of inference can be so rapid and unconscious that the researcher really “sees” the molecule in the NMR spectrum. For a biochemist or molecular biologist, the data are much more complex and the structural information emerges slowly through a process of computer-aided data analysis.

The goal of this book is to develop in the reader a real understanding of NMR and how it works. Many people who use NMR have no idea what the instrument does or how the experiments manipulate the nuclei of the molecule to reveal structural information. Because NMR is a technique involving the physics of magnetism and superconductivity, radio frequency electronics, digital data processing, and quantum mechanics of nuclear spins, many researchers are understandably intimidated and wish only to know “which button to push.” Although a simple list of instructions and an understanding of data interpretation are enough for many people, this book attempts to go deeper without getting buried in technical details and physical and mathematical formalism. It is my belief that with a relatively simple set of theoretical tools, learned by hands-on problem solving and experience, the organic chemist or biologist can master all of the modern NMR techniques with a solid understanding of how they work and what needs to be adjusted or optimized to get the most out of these techniques.

In this book we will start with a very primitive model of the NMR experiment, and explain the simplest NMR techniques using this model. As the techniques become more complex and powerful, we will need to expand this model one step at a time, each time avoiding formal physics and quantum mechanics as much as possible and instead relying on analogy and common sense. Necessarily, as the model becomes more sophisticated, the comfortable physical analogies become fewer, and we have to rely more on symbols and math. With lots of examples and frequent reminders of what the practical result (NMR spectrum) would be at each stage of the process, these symbols become familiar and useful tools. To understand NMR one only needs to look at the interaction of at most two nearby nuclei in a molecule,

so the theory will not be developed beyond this simplest of relationships. By the end of this book, you should be able to read the literature of new NMR experiments and be able to understand even the most complex biological NMR techniques. My goal is to make this rich literature accessible to the “masses” of researchers who are not experts in physics or physical chemistry. My hope is that this understanding, like all deep understanding of science, will be satisfying and rewarding and, in a research environment, empowering.

ACKNOWLEDGMENTS

I would like to thank my NMR mentors: Paul A. Bartlett (University of California, Berkeley), who taught me the beauty of natural product structure elucidation by NMR and chemical methods through group meeting problem sessions and graduate courses; Krish Krishnamurthy, who introduced me to NMR maintenance and convinced me of the power and usefulness of product operator formalism during a postdoc in John Casida's lab at Berkeley; Rachel E. Klevit (University of Washington), who gave me a great opportunity to get started in protein NMR; and Wayne J. Fairbrother (Genentech, Inc.), who taught me the highest standards of excellence and thoroughness in structural biology by NMR. Through this book I hope to pass on some of the knowledge that was so generously given to me.

This book grew out of my course in NMR spectroscopy that began in 1987 as an undergraduate course at The Evergreen State College, Olympia, WA, and continued in 1997 as a graduate course at the University of Arizona. Those who helped me along the way include Professors Michael Barfield, F. Ann Walker, and Michael Brown, as well as my teaching assistants, especially Igor Filippov, Jinfa Ying, and Liliya Yatsunyk.

1

FUNDAMENTALS OF NMR SPECTROSCOPY IN LIQUIDS

1.1 INTRODUCTION TO NMR SPECTROSCOPY

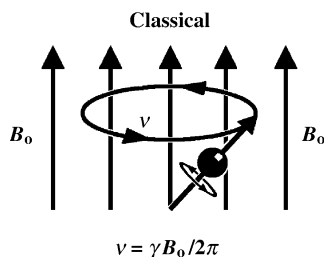
NMR is a spectroscopic technique that relies on the magnetic properties of the atomic nucleus. When placed in a strong magnetic field, certain nuclei resonate at a characteristic frequency in the radio frequency range of the electromagnetic spectrum. Slight variations in this resonant frequency give us detailed information about the molecular structure in which the atom resides.

1.1.1 The Classical Model

Many atoms (e.g., ^1H , ^{13}C , ^{15}N , ^{31}P) behave as if the positively charged nucleus was spinning on an axis (Fig. 1.1). The spinning charge, like an electric current, creates a tiny magnetic field. When placed in a strong external magnetic field, the magnetic nucleus tries to align with it like a compass needle in the earth's magnetic field. Because the nucleus is spinning and has angular momentum, the torque exerted by the external field results in a circular motion called precession, just like a spinning top in the earth's gravitational field. The rate of this precession is proportional to the external magnetic field strength and to the strength of the nuclear magnet:

$$\nu_0 = \gamma B_0 / 2\pi$$

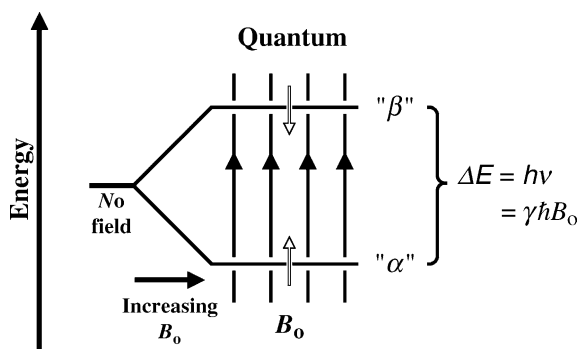
where ν_0 is the precession rate (the "Larmor frequency") in hertz, γ is the strength of the nuclear magnet (the "magnetogyric ratio"), and B_0 is the strength of the external magnetic field. This resonant frequency is in the radio frequency range for strong magnetic fields

**Figure 1.1**

and can be measured by applying a radio frequency signal to the sample and varying the frequency until absorbance of energy is detected.

1.1.2 The Quantum Model

This classical view of magnetic resonance, in which the nucleus is treated as a macroscopic object like a billiard ball, is insufficient to explain all aspects of the NMR phenomenon. We must also consider the quantum mechanical picture of the nucleus in a magnetic field. For the most useful nuclei, which are called “spin $\frac{1}{2}$ ” nuclei, there are two quantum states that can be visualized as having the spin axis pointing “up” or “down” (Fig. 1.2). In the absence of an external magnetic field, these two states have the same energy and at thermal equilibrium exactly one half of a large population of nuclei will be in the “up” state and one half will be in the “down” state. In a magnetic field, however, the “up” state, which is aligned with the magnetic field, is lower in energy than the “down” state, which is opposed to the magnetic field. Because this is a quantum phenomenon, there are no possible states in between. This energy separation or “gap” between the two quantum states is proportional to the strength of the external magnetic field, and increases as the field strength is increased. In a large population of nuclei in thermal equilibrium, slightly more than half will reside in the “up” (lower energy) state and slightly less than half will reside in the “down” (higher energy) state. As in all forms of spectroscopy, it is possible for a nucleus in the lower energy state to absorb a photon of electromagnetic energy and be promoted to the higher energy state. The energy of the photon must exactly match the energy “gap” (ΔE) between

**Figure 1.2**

the two states, and this energy corresponds to a specific frequency of electromagnetic radiation:

$$\Delta E = h\nu_0 = h\gamma B_0/2\pi$$

where h is Planck's constant. The resonant frequency, ν_0 , is in the radio frequency range, identical to the precession frequency (the Larmor frequency) predicted by the classical model.

1.1.3 Useful Nuclei for NMR

The resonant frequencies of some important nuclei are shown below for the magnetic field strength of a typical NMR spectrometer (Varian Gemini-200):

Nucleus	Abundance (%)	Sensitivity	Frequency (MHz)
^1H	100	1.0	200
^{13}C	1.1	0.016	50
^{15}N	0.37	0.001	20
^{19}F	100	0.83	188
^{31}P	100	0.066	81
^{57}Fe	2.2	3.4×10^{-5}	6.5

The spectrometer is a radio receiver, and we change the frequency to “tune in” each nucleus at its characteristic frequency, just like the stations on your car radio. Because the resonant frequency is proportional to the external magnetic field strength, all of the resonant frequencies above would be increased by the same factor with a stronger magnetic field. The relative sensitivity is a direct result of the strength of the nuclear magnet, and the effective sensitivity is further reduced for those nuclei that occur at low natural abundance. For example, ^{13}C at natural abundance is 5700 times less sensitive ($1/(0.011 \times 0.016)$) than ^1H when both factors are taken into consideration.

1.1.4 The Chemical Shift

The resonant frequency is not only a characteristic of the type of nucleus but also varies slightly depending on the position of that atom within a molecule (the “chemical environment”). This occurs because the bonding electrons create their own small magnetic field that modifies the external magnetic field in the vicinity of the nucleus. This subtle variation, on the order of one part in a million, is called the chemical shift and provides detailed information about the structure of molecules. Different atoms within a molecule can be identified by their chemical shift, based on molecular symmetry and the predictable effects of nearby electronegative atoms and unsaturated groups.

The chemical shift is measured in parts per million (ppm) and is designated by the Greek letter delta (δ). The resonant frequency for a particular nucleus at a specific position within a molecule is then equal to the fundamental resonant frequency of that isotope (e.g., 50.000 MHz for ^{13}C) times a factor that is slightly greater than 1.0 due to the chemical shift:

$$\text{Resonant frequency} = \nu(1.0 + \delta \times 10^{-6})$$

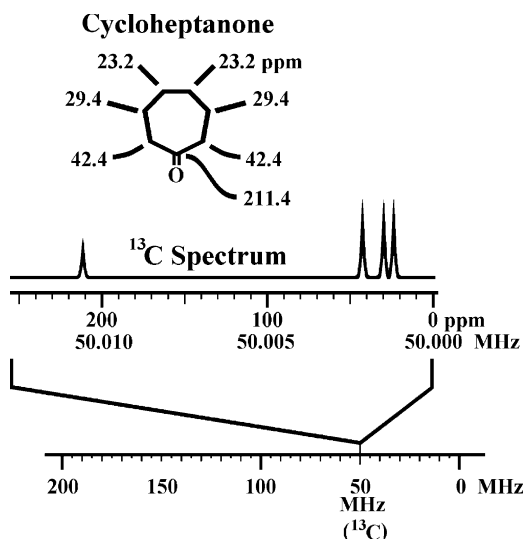


Figure 1.3

For example, a ^{13}C nucleus at the C-4 position of cycloheptanone ($\delta 23.3$ ppm) resonates at a frequency of

$$50.000 \text{ MHz} (1.0 + 23.2 \times 10^{-6}) = 50.000(1.0000232) = 50,001,160 \text{ Hz}$$

A graph of the resonant frequencies over a very narrow range of frequencies centered on the fundamental resonant frequency of the nucleus of interest (e.g., ^{13}C at 50.000 MHz) is called a *spectrum*, and each peak in the spectrum represents a unique chemical environment within the molecule being studied. For example, cycloheptanone has four peaks due to the four unique carbon positions in the molecule (Fig. 1.3). Note that symmetry in a molecule can make the number of unique positions less than the total number of carbons.

1.1.5 Spin-Spin Splitting

Another valuable piece of information about molecular structure is obtained from the phenomenon of spin-spin splitting. Consider two protons ($^1\text{H}_a\text{C}-\text{C}^1\text{H}_b$) with different chemical shifts on two adjacent carbon atoms in an organic molecule. The magnetic nucleus of H_b can be either aligned with (“up”) or against (“down”) the magnetic field of the spectrometer (Fig. 1.4). From the point of view of H_a , the H_b nucleus magnetic field perturbs the external magnetic field, adding a slight amount to it or subtracting a slight amount from it, depending on the orientation of the H_b nucleus (“up” or “down”). Because the resonant frequency is always proportional to the magnetic field *experienced* by the nucleus, this changes the H_a frequency so that it now resonates at one of two frequencies very close together. Because roughly 50% of the H_b nuclei are in the “up” state and roughly 50% are in the “down” state, the H_a resonance is “split” by H_b into a pair of resonance peaks of equal intensity (a “doublet”) with a separation of J Hz, where J is called the coupling constant. The relationship is mutual so that H_b experiences the same splitting effect (separation of J Hz) from H_a . This effect is transmitted through bonds and operates only when the two nuclei are very close (three bonds or less) in the bonding network. If there is more than one “neighbor”

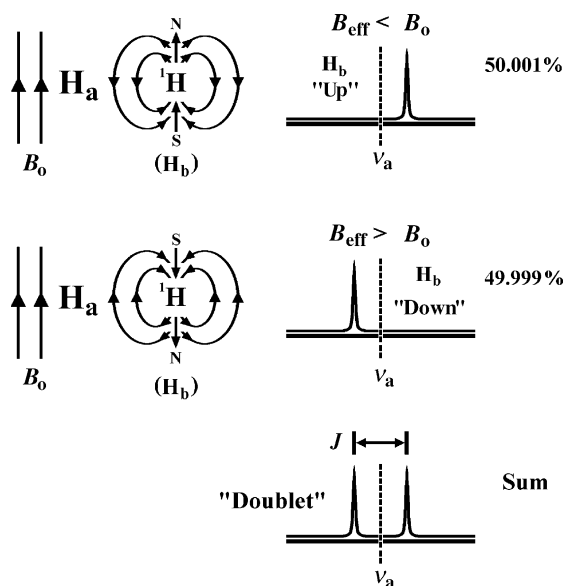


Figure 1.4

proton, more complicated splitting occurs so that the number of peaks is equal to one more than the number of neighboring protons doing the splitting. For example, if there are two neighboring protons ($H_aC-CH^b_2$), there are four possibilities for the H_b protons, just like the possible outcomes of flipping two coins: both "up," the first "up" and the second "down," the first "down" and the second "up," and both "down." If one is "up" and one "down" the effects cancel each other and the H_a proton absorbs at its normal chemical shift position (ν_a). If both H_b spins are "up," the H_a resonance is shifted to the right by J Hz. If both are "down," the H_a resonance occurs J Hz to the left of ν_a . Because there are two ways it can happen, the central resonance at ν_a is twice as intense as the outer resonances, giving a "triplet" pattern with intensity ratio 1 : 2 : 1 (Fig. 1.5). Similar arguments for larger numbers of neighboring spins lead to the general case of n neighboring spins, which split the H_a resonance peak into $n + 1$ peaks with an intensity ratio determined by *Pascal's triangle*. This triangle of numbers is created by adding each adjacent pair of numbers to get the value below it in the triangle:

singlet	1	(no neighbors)
doublet	1 1	(one neighbor)
triplet	1 2 1	(two neighbors)
quartet	1 3 3 1	(three neighbors)
quintet	1 4 6 4 1	(four neighbors)
sextet	1 5 10 10 5 1	(five neighbors)
septet	1 6 15 20 15 6 1	(six neighbors)

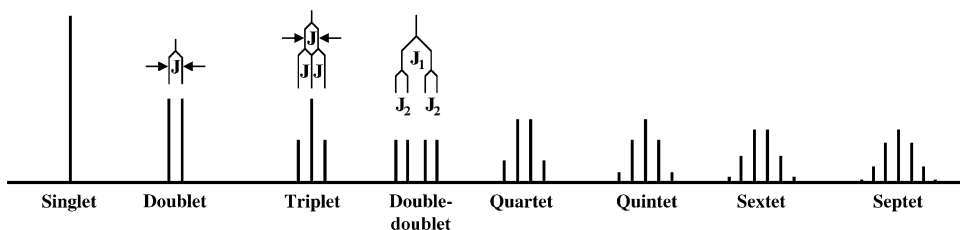


Figure 1.5

The strength of the spin–spin splitting interaction, measured by the peak separation (“ J value”) in units of hertz, depends in a predictable way on the dihedral angle defined by $H_a-C-C-H_b$, so that information can be obtained about the stereochemistry and conformation of molecules in solution. Because of this dependence on the geometry of the interceding bonds, it is possible to have couplings for two neighbors with different values of the coupling constant, J . This gives rise to a splitting pattern with four peaks of equal intensity: a double doublet (Fig. 1.5).

1.1.6 The NOE

A third type of information available from NMR comes from the nuclear Overhauser enhancement or NOE. This is a direct through-space interaction of two nuclei. Irradiation of one nucleus with a weak radio frequency signal at its resonant frequency will equalize the populations in its two energy levels. This perturbation of population levels disturbs the populations of nearby nuclei so as to enhance the intensity of absorbance at the resonant frequency of the nearby nuclei. This effect depends only on the distance between the two nuclei, even if they are far apart in the bonding network, and varies in intensity as the inverse sixth power of the distance. Generally the NOE can only be detected between protons (1H nuclei) that are separated by 5 \AA or less in distance. These measured distances are used to determine accurate three-dimensional structures of proteins and nucleic acids.

1.1.7 Pulsed Fourier Transform (FT) NMR

Early NMR spectrometers recorded a spectrum by slowly changing the frequency of a radio frequency signal fed into a coil near the sample. During this gradual “sweep” of frequencies the absorption of energy by the sample was recorded by a pen in a chart recorder. When the frequency passed through a resonant frequency for a particular nucleus in the sample, the pen went up and recorded a “peak” in the spectrum. This type of spectrometer, now obsolete, is called “continuous wave” or CW. Modern NMR spectrometers operate in the “pulsed Fourier-transform” (FT) mode, permitting the entire spectrum to be recorded in 2–3 s rather than the slow (5 min) frequency sweep. The collection of nuclei (sample) is given a strong radio frequency pulse that aligns the nuclei so that they precess in unison, each pointing in the same direction at the same time. The individual magnetic fields of the nuclei add together to give a measurable rotating magnetic field that induces an electrical voltage in a coil placed next to the sample. Over a period of a second or two the individual nuclei get out of synch and the macroscopic signal dies down. This “echo” of the pulse, observed in the coil, is called the free induction decay (FID), and it contains all of the resonant frequencies of the sample nuclei combined in one cacophonous reply. These data are digitised, and a

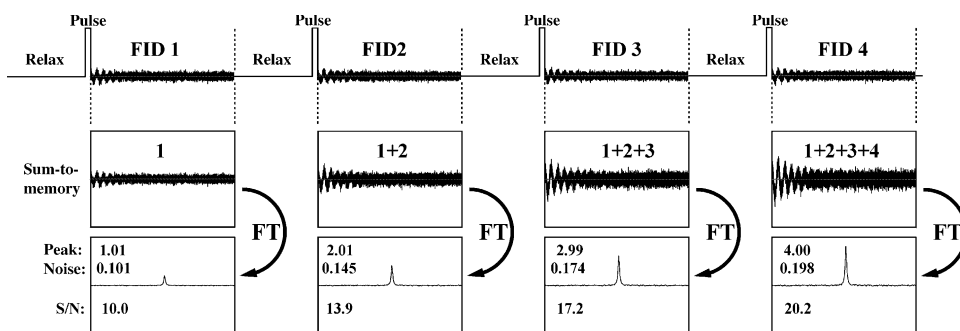


Figure 1.6

computer performs a Fast Fourier Transform to convert it from an FID signal as a function of time (time domain) to a plot of intensity as a function of frequency (frequency domain). The “spectrum” has one peak for each resonant frequency in the sample. The real advantage of the pulsed-FT method is that, because the data is recorded so rapidly, the process of pulse excitation and recording the FID can be repeated many times, each time adding the FID data to a sum stored in the computer (Fig. 1.6). The signal intensity increases in direct proportion to the number of repeats or “transients” (1.01, 2.01, 2.99, 4.00), but the random noise tends to cancel because it can be either negative or positive, resulting in a noise level proportional to the square root of the number of transients (0.101, 0.145, 0.174, 0.198). Thus the signal-to-noise ratio increases with the square root of the number of transients (10.0, 13.9, 17.2, 20.2). This signal-averaging process results in a vastly improved sensitivity compared to the old frequency sweep method.

The pulsed Fourier transform process is analogous to playing a chord on the piano and recording the signal from the decaying sound coming out of a microphone (Fig. 1.7). The chord consists of three separate notes: the “C” note is the lowest frequency, the “G” note is the highest frequency, and the “E” note is in the middle. Each of these pure frequencies gives a decaying pure sine wave in the microphone, and the combined signal of three frequencies is a complex decaying signal. This time domain signal (“FID”) contains all three of the frequencies of the piano chord. Fourier transform will then convert the data to a “spectrum”—a graph of signal intensity as a function of frequency, revealing the three frequencies of the chord as well as their relative intensities. The Fourier transform allows us to record all of the signals simultaneously and then “sort out” the individual frequencies later.

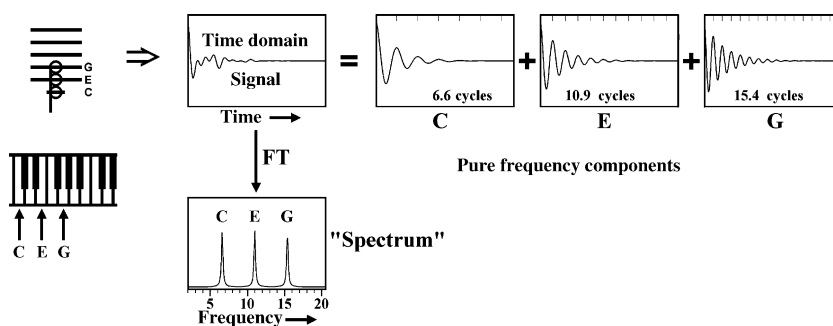


Figure 1.7

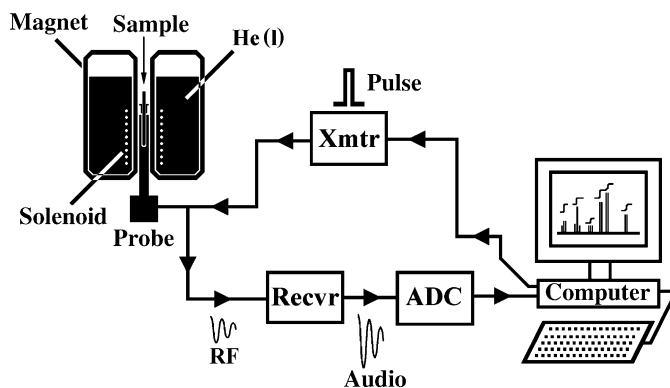


Figure 1.8

1.1.8 NMR Hardware

An NMR spectrometer consists of a superconducting magnet, a probe, a radio transmitter, a radio receiver, an analog-to-digital converter (ADC), and a computer (Fig. 1.8). The magnet consists of a closed loop (“solenoid”) of superconducting Nb/Ti alloy wire immersed in a bath of liquid helium (bp 4 K). A large current flows effortlessly around the loop, creating a strong continuous magnetic field with no external power supply. The helium can (“dewar”) is insulated with a vacuum jacket and further cooled by an outer dewar of liquid nitrogen (bp 77 K). The probe is basically a coil of wire positioned around the sample that alternately transmits and receives radio frequency signals. The computer directs the transmitter to send a high-power and very short duration pulse of radio frequency to the probe coil. Immediately after the pulse, the weak signal (FID) received by the probe coil is amplified, converted to an audio frequency signal, and sampled at regular intervals of time by the ADC to produce a digital FID signal, which is really just a list of numbers. The computer determines the timing and intensity of pulses output by the transmitter and receives and processes the digital information supplied by the ADC. After the computer performs the Fourier transform, the resulting spectrum can be displayed on the computer monitor and plotted on paper with a digital plotter. The cost of an NMR instrument is on the order of \$120,000–\$5,000,000, depending on the strength of the magnetic field (200–900 MHz proton frequency).

1.1.9 Overview of ^1H and ^{13}C Chemical Shifts

A general understanding of the trends of chemical shifts is essential for the interpretation of NMR spectra. The chemical shifts of ^1H and ^{13}C signals are affected by the proximity of electronegative atoms (O, N, Cl, etc.) in the bonding network and by the proximity to unsaturated groups (C=C, C=O, aromatic) directly through space. Electronegative groups shift resonances to the left (higher resonant frequency or “downfield”), whereas unsaturated groups shift to the left (downfield) when the affected nucleus is in the plane of the unsaturation, but have the opposite effect (shift to the right or “upfield”) in regions above and below this plane. Although the range of chemical shifts in parts per million is much larger for ^{13}C than for ^1H (0–220 ppm vs. 0–13 ppm), there is a rough correlation between the shift of a proton and the shift of the carbon it is attached to (Fig. 1.9). For a “hydrocarbon” environment with no electronegative atoms or unsaturated groups nearby, the shift is

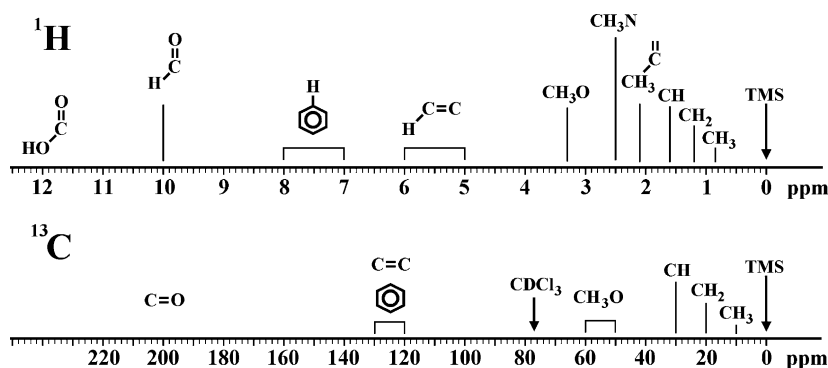


Figure 1.9

near the upfield (right) edge of the range, with a small downfield shift for each substitution: $\text{CH} > \text{CH}_2 > \text{CH}_3$ (^1H : 1.6, 1.2, 0.8; ^{13}C : 30, 20, 10 ppm). Oxygen has a stronger downfield-shifting effect than nitrogen due to its greater electronegativity: 3–4 ppm (^1H) and 50–85 (^{13}C) for CH-O . As with the hydrocarbon environment, the same downfield shifts are seen for increasing substitution: $\text{C}_q\text{-O}$ (quaternary) $>$ CH-O $>$ CH_2O $>$ CH_3O (^{13}C around 85, 75, 65, and 55 ppm, respectively). Proximity to an unsaturated group usually is downfield shifting because the affected atom is normally in the plane of the unsaturation: CH_3 attached to C=O moves downfield to 30 (^{13}C) and 2.1 ppm (^1H), whereas in HC=C (closer to the unsaturation) ^{13}C moves to 120–130 ppm and ^1H to 5–6 ppm. The combination of unsaturation *and* electronegativity is seen in H-C=O : 190 ppm ^{13}C and 10 ppm ^1H . There are some departures from this correlation of ^1H and ^{13}C shifts. Aromatic protons typically fall in the 7–8 ppm range rather than the 5–6 ppm range for olefinic (HC=C for an isolated C=C bond) protons, whereas ^{13}C shifts are about the same for aromatic or olefinic carbons. Because carbon has more than one bond, it is sensitive to distortion of its bond angles by the steric environment around it, with steric crowding usually leading to downfield shifts. Hydrogen has no such effect because it has only one bond, but it is more sensitive than carbon to the through-space effect of unsaturations. For example, converting an alcohol (CH-OH) to an ester (CH-OC(O)R) shifts the ^1H of the CH group downfield by 0.5 to 1 ppm, but has little effect on the ^{13}C shift.

1.1.10 Equivalence in NMR

Nuclei can be equivalent (have the same chemical shift) by symmetry within a molecule (e.g., the two methyl carbons in acetone, CH_3COCH_3), or by rapid rotation around single bonds (e.g., the three methyl protons in acetic acid, $\text{CH}_3\text{CO}_2\text{H}$). The intensity (integrated peak area or *integral*) of ^1H signals is directly proportional to the number of equivalent nuclei represented by that peak. For example, a CH_3 peak in a molecule would have three times the integrated peak area of a CH peak in the same molecule.

1.1.11 Proton Spectrum Example

The first step in learning to interpret NMR spectra is to learn how to predict them from a known chemical structure. An example of a ^1H (proton) NMR spectrum is shown for

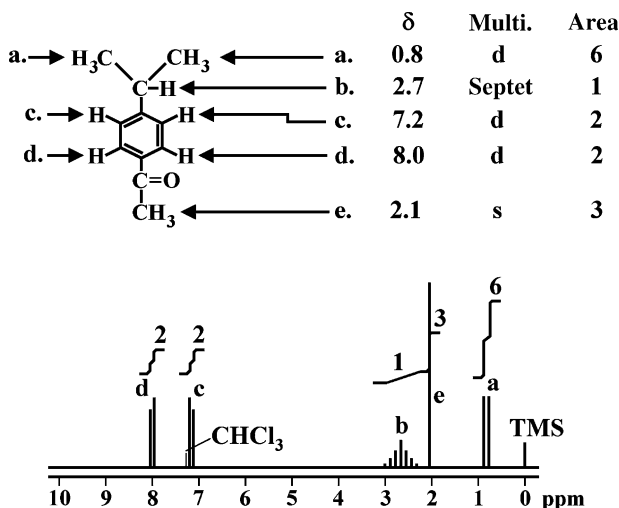


Figure 1.10

4-isopropylacetophenone (Fig. 1.10). The two isopropyl methyl groups are equivalent by symmetry, and each methyl group has three protons made equivalent by rapid rotation about the C–C bond. This makes all six H_a protons equivalent. Because they are far from any electronegative atom, these protons have a chemical shift typical of an isolated CH_3 group: 0.8 ppm (see Fig. 1.9). The absorbance is split into two peaks (a doublet) by the single neighboring H_b proton. The six H_a protons do not split each other because they are equivalent. The integrated area of the doublet is 6.0 because there are six H_a protons in the molecule. The H_b proton is split by all six of the H_a protons, so its absorbance shows up as a septet (seven peaks with intensity ratio 1:6:15:20:15:6:1). Its integrated area is 1.0, and its chemical shift is downfield of an isolated CH_2 (1.2 ppm) because of its proximity to the unsaturated aromatic ring (close to the plane of the aromatic ring so the effect is a downfield shift). The H_c methyl group protons are all equivalent due to rapid rotation of the CH_3 group, and their chemical shift is typical for a methyl group adjacent to the unsaturated $\text{C}=\text{O}$ group (2.1 ppm). There are no neighboring protons (the H_d proton is five bonds away from it, and the maximum distance for splitting is three bonds) so the absorbance appears as a single peak (“singlet”) with an integrated area of 3.0. The H_c and H_d protons on the aromatic ring appear at a chemical shift typical for protons bound directly to an aromatic ring, with the H_d protons shifted further downfield by proximity to the unsaturated $\text{C}=\text{O}$ group. Each pair of aromatic protons is equivalent due to the symmetry of the aromatic ring. The H_c absorbance is split into a doublet by the neighboring H_d proton (note that from the point of view of either of the H_c protons, only one of the H_d protons is close enough to cause splitting), and the H_d absorbance is split in the same way. Note that the J value (separation of split peaks) is the same for the H_c and H_d doublets, but slightly different for the H_a – H_b splitting. In this way we know, for example, that H_a is not split by either H_c or H_d .

1.1.12 Carbon Spectrum Example

The ^{13}C spectrum of the same compound is diagrammed in Figure 1.11. Several differences can be seen in comparison with the ^1H spectrum. First, there is no spin–spin splitting due

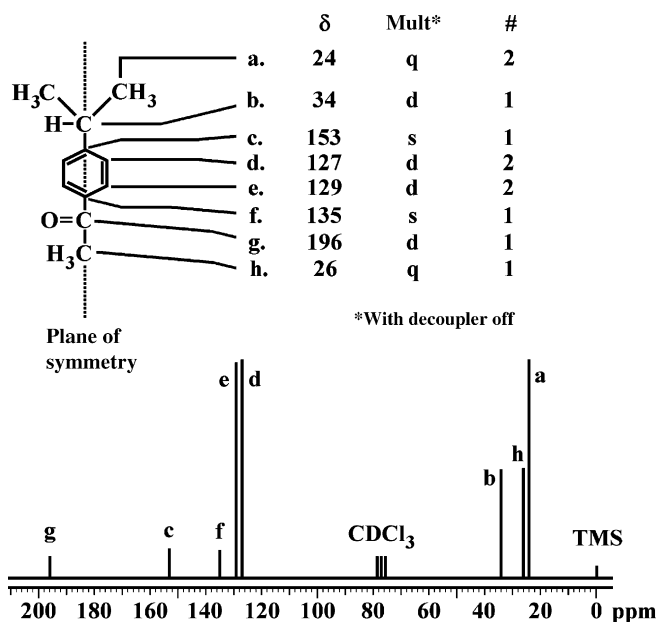


Figure 1.11

to adjacent carbons. This is because of the low natural abundance of ^{13}C , which is only 1.1%. Thus the probability of a ^{13}C occurring next to another ^{13}C is very low, and splitting is not observed because ^{12}C has no magnetic properties. Second, there is no spin-spin splitting due to the protons attached to each carbon. This is prevented intentionally by a process called *decoupling*, in which all the protons in the molecule are simultaneously irradiated with continuous low-power radio frequency energy at the proton resonance frequency. This causes each proton to flip rapidly between the upper and lower (disaligned and aligned) energy states, so that the ^{13}C nucleus sees only the average of the two states and appears as a singlet, regardless of the number of attached protons. The lack of any spin-spin splitting in decoupled ^{13}C spectra means that each carbon always appears as a singlet. The multiplicity (s, d, t, q) indicated for each carbon in the diagram is observed only with the decoupler turned off and is not shown in the spectrum. Third, the peaks are not integrated because the peak area does not indicate the number of carbon atoms accurately. This is because ^{13}C nuclei *relax* more slowly than protons, so that unless a very long relaxation delay between repetitive pulses is used, the population difference between the two energy states of ^{13}C is not reestablished before the next pulse arrives. Quaternary carbons, which have no attached protons, relax particularly slowly and thus show up with very low intensity.

The molecular symmetry, indicated by a dotted line (Fig. 1.11) where the mirror plane intersects the plane of the paper, makes the two isopropyl methyl carbons C_a equivalent. Their chemical shift is a bit downfield of an isolated methyl group due to the steric crowding of the isopropyl group. Unlike protons, ^{13}C nuclei are sensitive to the degree of substitution or branching in the immediate vicinity, generally being shifted downfield by increased branching. C_b is shifted further downfield because of direct substitution (it is attached to three other carbons) and proximity to the aromatic ring. C_h is in a relatively uncrowded

environment, but is shifted downfield by proximity to the unsaturated and electronegative carbonyl group. With the decoupler turned off, CH₃ carbons appear as quartets because of the three neighboring protons. The aromatic CH carbons C_d and C_e are in nearly identical environments typical of aromatic carbons, and each resonance peak represents two carbons due to molecular symmetry. With the decoupler turned off, these peaks turn into doublets due to the presence of a single attached proton. The two quaternary aromatic carbons C_c and C_f are shifted further downfield by greater direct substitution (they are attached to three other carbons) and by steric crowding (greater remote substitution) in the case of C_c and proximity to a carbonyl group in the case of C_f. The chemical shift of the carbonyl carbon C_g is typical for a ketone. All three of the quaternary carbons C_c, C_f, and C_g have low peak intensities due to slow relaxation (reestablishment of population difference) in the absence of directly attached protons.

1.2 EXAMPLES: NMR SPECTROSCOPY OF OLIGOSACCHARIDES AND TERPENOIDS

A few real-world examples will illustrate the use of ¹H and ¹³C chemical shifts and *J* couplings, as well as introduce some advanced methods we will use later. Two typical classes of complex organic molecules will be introduced here to familiarize the reader with the elements of structural organic chemistry that are important in NMR and how they translate into NMR spectra. Terpenoids are typical of natural products; they are relatively nonpolar (water insoluble) molecules with a considerable amount of “hydrocarbon” part and only a few functional groups—olefin, alcohol, ketone—in a rigid structure. Oligosaccharides are polar (water soluble) molecules in which every carbon is functionalized with oxygen—alcohol, ketone, or aldehyde oxidation states—and relatively rigid rings are connected with flexible linkages. In both cases, rigid cyclohexane-chair ring structures are ideal for NMR because they allow us to use *J*-coupling values to determine stereochemical relationships of protons (*cis* and *trans*). The molecules introduced here will be used throughout the book to illustrate the results of the NMR experiments.

1.2.1 Oligosaccharides

A typical monosaccharide (single carbohydrate building block) is a five or six carbon molecule with one of the carbons in the aldehyde or ketone oxidation state (the “anomeric” carbon) and the rest in the alcohol oxidation state (CH(OH) or CH₂OH). Thus the anomeric carbon is unique within the molecule because it has two bonds to oxygen whereas all of the other carbons have only one bond to oxygen. Normally the open-chain monosaccharide will form a five- or six-membered ring as a result of the addition of one of the alcohol groups (usually the second to last in the chain) to the ketone or aldehyde, changing the C=O double bond to an OH group.

The six-membered ring of glucose prefers the chair conformation shown in Figure 1.12, with nearly all of the OH groups arranged in the equatorial positions (sticking out and roughly in the plane of the ring) with the less bulky H atoms in the axial positions (pointing up or down, above or below the plane of the ring). This limits the dihedral angles between neighboring protons (vicinal or three-bond relationships) to three categories: axial–axial (*trans*): 180° dihedral angle, large *J* coupling (~10 Hz); axial–equatorial (*cis*): 60° dihedral angle, small *J* (~4 Hz); and equatorial–equatorial (*trans*): 60° dihedral angle, small *J* (~4 Hz).